

# Synthesis, Characterization and DNA-Binding Studies of Hydroxyl Functionalized Platinum(II) Salphen Complexes

Shahratul Ain Mohd Sukri<sup>1</sup> · Lee Yook Heng<sup>1</sup> · Nurul Huda Abd Karim<sup>1</sup>

Received: 23 January 2016 / Accepted: 3 February 2017  
© Springer Science+Business Media New York 2017

**Abstract** The platinum(II) salphen complex *N,N'*-Bis-4-(hydroxysalicylidene)-phenylenediamine-platinum(II); (**1**) and its two derivatives containing hydroxyl functionalized side chains *N,N'*-bis-[4-[[1-(2-hydroxyethoxy)] salicylidene] phenylenediamine-platinum(II); (**2**) and *N,N'*-bis-[4-[[1-(3-hydroxypropoxy)] salicylidene] phenylenediamine-platinum(II); (**3**) were synthesized and characterized. The structures of the complexes were confirmed by <sup>1</sup>H and <sup>13</sup>C NMR spectroscopy, FTIR, ESI-MS and CHN elemental analyses. The effects of the hydroxyl substituent on the spectral properties and the DNA binding behaviors of the Pt(II) complexes were explored. The binding mode and interactions of these complexes with duplex DNA (calf thymus DNA and porcine DNA) and also single-stranded DNA were studied by UV-Vis and emission DNA titration. The complexes interact with DNA by intercalation binding mode with the binding constants in the order of magnitude ( $K_b = 10^4 \text{ M}^{-1}$ , CT-DNA) and ( $K_b = 10^5 \text{ M}^{-1}$ , porcine DNA). The intercalation of the complex in the DNA structure was proposed to happen by  $\pi$ - $\pi$  stacking due to its square-planar geometry and aromatic rings structure. The phosphorescence emission spectral characteristics of Pt(II) complexes when interacted with DNA have been studied. Also, the application of the chosen hydroxypropoxy side chains complex (**3**) as an optical DNA biosensor, specifically for porcine DNA was investigated. These findings will

be valuable for the potential use of the platinum(II) salphen complex as an optical DNA biosensor for the detection of porcine DNA in food products.

**Keywords** Platinum(II) salphen · Phosphorescence complex · Calf thymus DNA · Porcine DNA · DNA binding · Optical DNA biosensor

## Introduction

Transition metal complexes have been established to have great ability to interact non-covalently with deoxyribonucleic acids (DNA) via different mechanism such as intercalation, groove binding or external electrostatic binding [1]. It is very important to conduct binding studies of small molecules to DNA for the development of new DNA molecular probes and therapeutic reagents [2].

Schiff base salphen ligand "*N,N'*-phenylenebis(salicylideneimine)" complexes have shown such strong DNA binding properties [3–5]. The interactions of square-planar and square-pyramidal metal-salphen complexes with duplex DNA and human telomeric quadruplex DNA have been studied by Vilar et al. in which the results highlighted that square-planar metal-salphen complexes are much more excellent quadruplex DNA stabilizer and binder due to its planar geometry structures which can provide optimal binding for  $\pi$ - $\pi$  stacking with the DNA [3]. Moreover, the metal center in salphen complexes plays important roles in "organizing" the salphen ligands into specific geometrical conformations ideally suited to  $\pi$ - $\pi$  stack onto the DNA (e.g.: square-planar and square-based pyramidal geometries) [4]. Metal center also have an important electronic role of "pulling" electrons from coordinated aromatic salphen ligands, thus making them more electron-deficient and

**Electronic supplementary material** The online version of this article (doi:10.1007/s10895-017-2035-0) contains supplementary material, which is available to authorized users.

✉ Nurul Huda Abd Karim  
nurulhuda@ukm.edu.my

<sup>1</sup> School of Chemical Sciences and Food Technology, Faculty of Science and Technology, Universiti Kebangsaan Malaysia, 43600 Bangi, Selangor, Malaysia

therefore more likely to be involved in  $\pi$ - $\pi$  interactions with the DNA nucleobases [4]. Other Schiff bases can have different types of binding modes with duplex DNA, for instance nickel salen [6], copper and zinc Schiff base complexes [7] which can interact with the double helix surface by means of intercalation and groove binding, respectively.

Platinum complex is highly phosphorescent [8] and widely used in optical devices and have diverse applications in electroluminescence, photovoltaics, optical limiting, photocatalysis, and molecular probes [9]. In addition, platinum has recently gained much attention in materials science and display technology since the discovery of highly efficient phosphorescent organic light-emitting diodes (OLEDs) based on platinum(II) complexes [10]. Moreover,  $d^8$  square-planar platinum(II) complexes with NN or CN bidentate; NNN, CNN or NCN terdentate; and NNNN or ONNO tetradentate conjugated aromatic ligands have shown to be highly phosphorescent at room temperature and widely used in OLEDs and in oxygen ( $O_2$ ) sensors [8]. It was also reported that the platinum(II) metal-salphen complexes have square-planar coordination geometry around the metal cation, which can enhance the  $\pi$ - $\pi$  stacking and increase the binding affinity with the DNA [5]. In this study, we decided to synthesis an emissive metal-salphen complex that can strongly bind to DNA. This complex will then be used as an optical indicator for DNA biosensor. Despite the fact that the platinum metal complexes' high optical properties could further enhance spectroscopic studies of DNA binding, no attempts have been made to explore the potential of the platinum(II) salphen complex as a new optical DNA indicator sensor material for DNA biosensor. Therefore, it has become our interest to investigate this matter.

Pork is a potential adulterant in food especially in meatballs and sausages due to its availability at cheaper prices. The mixing of pork or its derivatives in foods is a serious matter as it is not permissible by certain religious laws. In addition, unconscious consumption of pork may also cause allergic reactions in some individuals. It contains high levels of cholesterol and saturated fats that can be especially harmful for people with diabetes and cardiovascular disease [11]. Thus, the identification of pork in foods is very important for meat authentication and for meeting consumers' demand for protection against falsely labeled foods. In this regard, reliable methods for identification of porcine derivatives in food products are necessary for the analysis of food ingredients.

Current practice is to use the polymerase chain reaction (PCR) method for detection of porcine DNA in food products. This is the most common and effective method because it offers high levels of sensitivity [12]. Unfortunately, this method is time-consuming, tedious, and can only be run by skilled technicians [13, 14]. An alternative to this conventional PCR method is to develop porcine DNA biosensors that can offer an easy, rapid and simpler verification method of pork content

in food products such as, for instance, the gold nanoparticle sensor recently developed by Ali et al. [13]. Moreover, metal complex-based sensors could provide the advantage that the measurements can easily be run using optical instruments such as UV-Vis and fluorescence spectroscopy that are readily available in a chemical laboratory.

DNA-intercalation spectroscopy has been a particular interest among researchers. This is because many intercalators-DNA binding agents have very important functions such as anticancer drugs [15], photocleavage agents [16], DNA structure probes [17–19] and molecular DNA light switches [20, 21]. From the DNA binding spectroscopy studies, the binding mechanism and the detailed structure of the binding behavior properties obtained can be used to target specific sequence of DNA structures in order to develop a potential anticancer drugs or DNA molecular probes [15, 22–26], in which many of these functions based on the DNA-intercalation mechanism [23–26].

The molecular DNA light switches properties of the ruthenium(II) and cobalt(II) polypyridyl complexes were also determined from the DNA-intercalation spectroscopy studies of the complexes upon binding with the given DNA structures. These complexes showed a remarkable and intense luminescence and fluorescence enhancement in the presence of DNA, but lacks of luminescence and fluorescence in the absence of DNA due to its intercalation DNA binding properties, where it can be further use as fluorescence DNA probes or sensors [20, 21, 23, 27–29].

Moreover, DNA-intercalators binding molecules are also widely used in the design of optical DNA biosensors. For example, fluorescence dyes intercalators such as ethidium bromide (EB), acridine orange (AO) and thiazole orange (TO) and also metallointercalator such as ruthenium(II) polypyridine complex,  $[Ru(bpy)_2(dppz)]^{2+}$  [30–35]. These fluorescence intercalators act as an optical DNA hybridization indicators to detect the DNA hybridization event in the duplex DNA formed between the two DNA strands that are complementary to each other [32, 33, 36]. The intercalators will only produce fluorescence signals in the presence of hybridized DNA after intercalation of the binding molecules into the conjugated bases of the duplex DNA has occurred [31–33, 37]. These fibre-optic DNA biosensors are based on the monitoring of fluorescence signal that is emitted from the fluorescence intercalator-DNA binding agents, to show that hybridization of DNA has been formed between the probe DNA sequence and the target DNA sequence [32, 33]. The complimentary oligonucleotide that have undergo DNA hybridization will show an enhancement of fluorescence signal while the non-complimentary oligonucleotide without any hybridization will not show any enhancement of fluorescence signal [36]. Since intercalators-DNA binding molecules have such great potential as optical DNA biosensors, we are greatly interested to study the DNA binding properties of the platinum(II) salphen

complexes and investigate its potential application as an optical indicator sensor material for DNA biosensor.

We report herein the synthesis, characterization, and DNA binding properties of two platinum(II) salphen complexes with the hydroxyl functionalized side chains substituent on their salphen ligand core. The complexes' interactions with DNA are studied to determine whether it can act as an intercalator agent due to its planar aromatic rings structure [38]. This paper is focused on exploring the effects of the hydroxyl substituents (with varying lengths of the alkoxy side chain arms) on the spectral properties and DNA binding behaviors of the complexes. The need to vary different substituents on the ligand is because it can create some differences in the space configuration and also the electron density distribution of the complexes, therefore variation in the spectral properties and different DNA binding behaviors of the complexes can be obtained [39]. Additionally, the binding affinities and selectivity of the platinum(II) salphen complexes towards duplex porcine DNA over single-stranded DNA (represented by beef ssDNA) and CT-DNA are determined, with their duplex and single-stranded DNA affinities reported herein. The strong binding affinity and high selectivity of the complex towards porcine DNA is established in this work, so that it can be used as a potential porcine DNA biosensor. We also show that the platinum(II) complexes in this work are emissive, which inspire us to carry out optical phosphorescence DNA selectivity study as a preliminary sensor studies for the potential use of the complex as an optical indicator sensor material for porcine DNA biosensor, which can be used in future food industry analysis. Studies on the DNA binding of these complexes are very important in the development of new fluorescence (or phosphorescence) optical DNA sensors and DNA molecular probes. Therefore, it is important that we need to establish the binding mode and affinity of the potential metal complexes to porcine DNA first, and choose the best metal complex intercalator before we fabricate the optical indicator onto solid support for the development of porcine DNA biosensor in our future works.

## Experimental

### Materials, Methods and Instrumentation

Analytical grade reagents and chemicals were obtained from Sigma Aldrich Chemical Co. (USA). Single-stranded porcine DNA corresponding to the 25 nt complimentary target porcine sequence 567-(5')-TAC CGC CCT CGC AGC CGT ACA TCT C-(3')-591 of the *Sus scrofa* cytochrome b (cytb) gene, its probe porcine sequence strand (3')-ATG GCG GGA GCG TCG GCA TGT AGA G-(5'), calf thymus-DNA (CT-DNA) and the single-stranded DNA (non-complimentary DNA strands) (a) *Bos taurus* cytb (beef ssDNA) 567- (5')-CAT

AGC AAT TGC CAT AGT CCA CCT A-(3')-591, (b) *Gallus gallus* cytb (chicken ssDNA) 567- (5')-CGC AGG TAT TAC TAT CAT CCA CCT C-(3')-591 were obtained from Sigma (USA).  $^1\text{H}$  and  $^{13}\text{C}$  NMR spectra were recorded on a Bruker AVANCE III 600 MHz spectrometer equipped with a cryoprobe. Infrared Spectra were recorded on a Perkin-Elmer FTIR 1720 spectrometer as KBr discs between 4000 and  $400\text{ cm}^{-1}$ . Elemental analyses were recorded on a Thermo Finnigan EA 1112 CHNS. UV-Vis spectra were recorded in 1 cm path length quartz cuvettes using a Perkin Elmer Lambda 25 UV-Vis spectrometer. Emission DNA titration were recorded in 1 cm path length quartz cuvettes using a Perkin Elmer LS55 Luminescence Spectrophotometer at a scan rate of 200 nm/min. The slit width was 5 nm for both excitation and emission. The excitation wavelength used was 370 nm. The emitted light was collected at an angle of  $90^\circ$  relative to the excitation light.

### General Procedure<sup>1</sup>

#### *Synthesis of Salphen Ligand: N,N'-Bis-4-(Hydroxysalicylidene)-Phenylenediamine*

The salphen ligand was prepared using a condensation reaction of *o*-phenylenediamine with 2,4-dihydroxybenzaldehyde in a 1:2 M ratio in ethanol. The mixture of 2,4-dihydroxybenzaldehyde (0.22 g, 1.60 mmol) and 1,2-phenylenediamine (0.09 g, 0.80 mmol) in ethanol was refluxed at  $79^\circ\text{C}$  for 4 h. The ethanol was evaporated under reduced pressure. The resulting solid was washed with diethyl ether and water and collected by filtration to obtain the salphen ligand as a yellow-orange precipitate. Yield: 0.12 g (45%). IR (KBr pellet)/ $\text{cm}^{-1}$ : 3063 (C-H aromatic), 1609 (C = N), 1574 (C = C aromatic), 1546 (C = C aromatic), 1502 (C = C aromatic), 1209 (C-O), 1123 (C-O).  $^1\text{H}$  NMR (600 MHz, DMSO- $d_6$ ):  $\delta$  13.38 (s, 1H, H<sup>8</sup>, -OH phenol), 10.26 (s, 1H, H<sup>7</sup>, -OH phenol), 8.75 (s, 1H, H<sup>3</sup>, N = C-H), 7.43 (d,  $^3J_{\text{HH}} = 9\text{ Hz}$ , 1H, H<sup>4</sup>, Ar-H), 7.38(dd,  $^3J_{\text{HH}} = 6\text{ Hz}$ ,  $^4J_{\text{HH}} = 3.6\text{ Hz}$ , 1H, H<sup>2</sup>, Ar-H), 7.32 (dd,  $^3J_{\text{HH}} = 6\text{ Hz}$ ,  $^4J_{\text{HH}} = 3\text{ Hz}$ , 1H, H<sup>1</sup>, Ar-H), 6.39 (dd,  $^3J_{\text{HH}} = 8.4\text{ Hz}$ ,  $^4J_{\text{HH}} = 2.4\text{ Hz}$ , 1H, H<sup>5</sup>, Ar-H), 6.28 (d,  $^4J_{\text{HH}} = 2.4\text{ Hz}$ , 1H, H<sup>6</sup>, Ar-H).  $^{13}\text{C}$  NMR (600 MHz, DMSO- $d_6$ ):  $\delta$  163.80, 163.39, 163.09, 142.28, 134.91, 127.52, 119.95, 112.76, 108.30, 102.87 ppm. ESI-MS calculated for  $\text{C}_{20}\text{H}_{16}\text{N}_2\text{O}_4$  (M)<sup>+</sup>: 348.36 a.m.u. Found: 349.09 a.m.u. Anal. Calc. for  $\text{C}_{20}\text{H}_{16}\text{N}_2\text{O}_4$ : C 68.96, H 4.63, N 8.04. Found: C 67.69, H 4.58, N 8.03%.

<sup>1</sup> Chemical shift in units of parts-per-million, ppm ( $\delta$ ), proton-proton coupling constants ( $J_{\text{HH}}$ ), dimethyl sulfoxide (DMSO).

*Synthesis of Platinum(II) Salphen Complex: N,N'-Bis-4-(Hydroxysalicylidene)-Phenylenediamine-Platinum(II) (1)*

The synthesis of the platinum salphen complex was carried out using the method described by Wu et al. [9] and Zhou et al. [8] with slight modifications. The salphen ligand (0.28 g, 0.80 mmol) was dissolved in 30 mL acetonitrile and sodium acetate which act as a base was added to the salphen ligand mixture and stirred for 5 min. Potassium tetrachloroplatinate (0.66 g, 1.60 mmol) in DMSO (2 mL) was added and stirred at 30 °C for 72 h. The solid was then filtered and washed with diethyl ether and water to obtain the platinum(II)-salphen complex as an orange-brownish precipitate. Yield: 0.09 g (22%). IR (KBr pellet)/cm<sup>-1</sup>: 3368 (OH alcohol/phenol), 3066 (C-H aromatic), 1601 (C = N), 1581 (C = C aromatic), 1545 (C = C aromatic), 1493 (C = C aromatic), 1440 (C = C aromatic), 1180 (C-O), 1128 (C-O). <sup>1</sup>H NMR (600 MHz, DMSO-d<sub>6</sub>): δ 10.50 (s, 1H, H<sup>7</sup>, -OH phenol), 9.19 (s, 1H, H<sup>3</sup>, N = C-H), 8.30 (dd, <sup>3</sup>J<sub>HH</sub> = 6 Hz, <sup>4</sup>J<sub>HH</sub> = 3.6 Hz, 1H, H<sup>2</sup>, Ar-H), 7.66 (d, <sup>3</sup>J<sub>HH</sub> = 8.4 Hz, 1H, H<sup>4</sup>, Ar-H), 7.34 (dd, <sup>3</sup>J<sub>HH</sub> = 6.3 Hz, <sup>4</sup>J<sub>HH</sub> = 3.3 Hz, 1H, H<sup>1</sup>, Ar-H), 6.44 (d, <sup>4</sup>J<sub>HH</sub> = 2.4 Hz, 1H, H<sup>6</sup>, Ar-H), 6.34 (dd, <sup>3</sup>J<sub>HH</sub> = 8.7 Hz, <sup>4</sup>J<sub>HH</sub> = 2.1 Hz, 1H, H<sup>5</sup>, Ar-H). <sup>13</sup>C NMR (600 MHz, DMSO-d<sub>6</sub>): δ 166.93, 165.03, 149.79, 144.83, 137.81, 127.30, 116.61, 108.98, 104.76. ESI-MS calculated for C<sub>20</sub>H<sub>14</sub>N<sub>2</sub>PtO<sub>4</sub> (M + Na)<sup>+</sup>: 564.41 a.m.u. Found: 564.05 a.m.u. Anal. Calc. for C<sub>20</sub>H<sub>14</sub>N<sub>2</sub>PtO<sub>4</sub> · 3H<sub>2</sub>O: C 40.34, H 3.38, N 4.70. Found: C 40.40, H 3.51, N 3.48%.

*Synthesis of Platinum(II) Salphen Complex Hydroxyl Functionalized Derivative: N,N'-Bis-4-[[1-(2-Hydroxyethoxy)] Salicylidene] Phenylenediamine-Platinum (II) (2)*

The synthesis of the platinum salphen complex hydroxyl side chains derivative was carried out by a slight modification from the methods described by Vilar et al. [3] The platinum(II) salphen complex (0.32 g, 0.58 mmol) was reacted with 2-chloro-1-ethanol (199.42 μL, 2.98 mmol) and potassium carbonate (0.66 g, 4.76 mmol). It was stirred at 90 °C for 72 h in DMF solvent (30 mL). After this period of time the salts were removed by filtration and the DMF was evaporated under reduced pressure. The resulting solid was washed with water and n-hexane to yield a dark brown precipitate. Yield: 0.05 g (15%). IR (KBr pellet)/cm<sup>-1</sup>: 3369 (OH alcohol/phenol), 2916 (C-H alkane), 1603 (C = N), 1578 (C = C aromatic), 1521 (C = C aromatic), 1458 (C = C aromatic), 1421 (C = C aromatic), 1188 (C-O), 1129 (C-O), 1026 (C-O ether). <sup>1</sup>H NMR (600 MHz, DMSO-d<sub>6</sub>): δ 9.29 (s, 1H, H<sup>3</sup>, N = C-H), 8.34 (dd, <sup>3</sup>J<sub>HH</sub> = 6 Hz, <sup>4</sup>J<sub>HH</sub> = 3.6 Hz, 1H, H<sup>2</sup>, Ar-H), 7.73 (d, <sup>3</sup>J<sub>HH</sub> = 8.4 Hz, 1H, H<sup>4</sup>, Ar-H), 7.36 (dd, <sup>3</sup>J<sub>HH</sub> = 6.3 Hz, <sup>4</sup>J<sub>HH</sub> = 3.3 Hz, 1H, H<sup>1</sup>, Ar-H), 6.59 (d, <sup>4</sup>J<sub>HH</sub> = 2.4 Hz, 1H,

H<sup>6</sup>, Ar-H), 6.47 (dd, <sup>3</sup>J<sub>HH</sub> = 8.7 Hz, <sup>4</sup>J<sub>HH</sub> = 2.1 Hz, 1H, H<sup>5</sup>, Ar-H), 4.97 (s, 1H, H<sup>13</sup>, -OH), 4.08 (t, 2H, H<sup>11</sup>, -CH<sub>2</sub>), 3.76 (t, 2H, H<sup>12</sup>, -CH<sub>2</sub>). <sup>13</sup>C NMR (600 MHz, DMSO-d<sub>6</sub>): δ 166.80, 165.44, 149.90, 144.71, 137.28, 127.62, 116.93, 116.63, 108.64, 103.03, 70.20, 59.85. ESI-MS calculated for C<sub>24</sub>H<sub>22</sub>N<sub>2</sub>PtO<sub>6</sub> (M + K)<sup>+</sup>: 668.49 a.m.u. Found: 668.07 a.m.u.

*Synthesis of Platinum(II) Salphen Complex Hydroxyl Functionalized Derivative: N,N'-Bis-4-[[1-(3-Hydroxypropoxy)] Salicylidene] Phenylenediamine-Platinum(II) (3)*

The synthesis of the platinum salphen complex hydroxyl side chains derivative was carried out by a slight modification from the methods described by Vilar et al. [3] The platinum(II) salphen complex (0.27 g, 0.49 mmol) was reacted with 3-chloro-1-propanol (206.05 μL, 2.47 mmol) and potassium carbonate (0.55 g, 3.94 mmol). It was stirred at 90 °C for 72 h in DMF solvent (30 mL). After this period of time the salts were removed by filtration and the DMF was evaporated under reduced pressure. The resulting solid was washed with water to yield a dark brown precipitate. Yield: 0.11 g (35%). IR (KBr pellet)/cm<sup>-1</sup>: 3400 (OH alcohol/phenol), 2916 (C-H alkane), 1603 (C = N), 1578 (C = C aromatic), 1517 (C = C aromatic), 1463 (C = C aromatic), 1420 (C = C aromatic), 1189 (C-O), 1129 (C-O), 1024 (C-O ether). <sup>1</sup>H NMR (600 MHz, DMSO-d<sub>6</sub>): δ 9.27 (s, 1H, H<sup>3</sup>, N = C-H), 8.34 (dd, <sup>3</sup>J<sub>HH</sub> = 6 Hz, <sup>4</sup>J<sub>HH</sub> = 3.6 Hz, 1H, H<sup>2</sup>, Ar-H), 7.71 (d, <sup>3</sup>J<sub>HH</sub> = 8.4 Hz, 1H, H<sup>4</sup>, Ar-H), 7.37 (dd, <sup>3</sup>J<sub>HH</sub> = 6.3 Hz, <sup>4</sup>J<sub>HH</sub> = 3.3 Hz, 1H, H<sup>1</sup>, Ar-H), 6.58 (d, <sup>4</sup>J<sub>HH</sub> = 2.4 Hz, 1H, H<sup>6</sup>, Ar-H), 6.45 (dd, <sup>3</sup>J<sub>HH</sub> = 8.7 Hz, <sup>4</sup>J<sub>HH</sub> = 2.1 Hz, 1H, H<sup>5</sup>, Ar-H), 4.63 (s, 1H, H<sup>14</sup>, -OH), 4.13 (t, 2H, H<sup>11</sup>, -CH<sub>2</sub>), 3.58 (t, 2H, H<sup>13</sup>, -CH<sub>2</sub>), 1.90 (m, 2H, H<sup>12</sup>, -CH<sub>2</sub>). <sup>13</sup>C NMR (600 MHz, DMSO-d<sub>6</sub>): δ 166.92, 165.46, 150.03, 144.71, 137.27, 127.62, 116.93, 116.71, 108.69, 103.00, 65.32, 57.69, 32.32. ESI-MS calculated for C<sub>26</sub>H<sub>26</sub>N<sub>2</sub>PtO<sub>6</sub> (M + K)<sup>+</sup>: 696.54 a.m.u. Found: 696.07 a.m.u.

*DNA Binding Experiments*

Single-stranded porcine DNA, corresponding to the 25 nt probe sequence (3')-ATG GCG GGA GCG TCG GCA TGT AGA G-(5') of the *Sus scrofa* cytochrome b (cytb) gene and its complementary strand 567-(5')-TAC CGC CCT CGC AGC CGT ACA TCT C-(3')-591 were dissolved in the 10 mM Tris-HCl buffer at pH 7.4 to yield a 2 mM solution. Both single-stranded DNA fragments were annealed by heating to 90 °C for 5 min and then cooled to room temperature overnight to form duplex porcine DNA. The stock solution of CT-DNA was prepared by dissolving it in the 10 mM Tris-HCl buffer at pH 7.4. The ratio of the absorbance of CT-DNA solution at 260 nm and 280 nm was 1.9, which is more than 1.8, indicating that CT-DNA was not contaminated by proteins [40]. The

concentration of CT-DNA was calculated from its absorption intensity at 260 nm using a molar absorption coefficient value of  $6600 \text{ M}^{-1} \text{ cm}^{-1}$  [41]. Excitation wavelengths of 370 nm were used for DNA emission titration studies. For DNA selectivity studies, the single-stranded DNA (non-complementary DNA strands) used are: a) *Bos taurus* cytb (beef ssDNA) 567- (5')-CAT AGC AAT TGC CAT AGT CCA CCT A-(3')-591 and b) *Gallus gallus* cytb (chicken ssDNA) 567- (5')-CGC AGG TAT TAC TAT CAT CCA CCT C-(3')-591 [13].

## Results and Discussion

### Synthesis and Characterization of Platinum(II) Salphen Complex and Its Hydroxyl Side Chains Derivatives

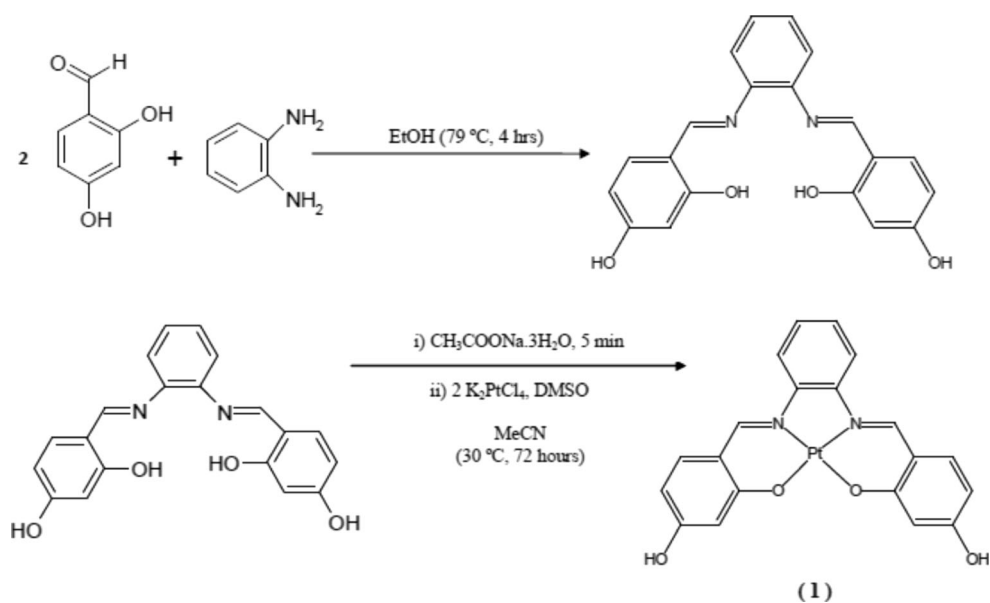
The platinum(II) salphen complex was synthesized via condensation reaction of 2,4-dihydroxybenzaldehyde and *o*-phenylenediamine with potassium tetrachloroplatinate to obtain *N,N'*-Bis-4-(hydroxysalicylidene)-phenylenediamine-platinum(II); non-side chains complex (**1**). The reaction schemes for the synthesis of salphen ligand and its platinum(II) salphen complex are illustrated in Fig. 1.

The signal of the aldehyde proton at 9.92 ppm is absent in the  $^1\text{H}$  NMR spectrum of the salphen ligand which confirms that the aldehyde group of the starting compound 2,4-dihydroxybenzaldehyde has been converted to N = C-H imine group. Moreover, the  $^1\text{H}$  NMR spectrum of the salphen ligand displays correct integration and multiplets pattern (supplementary data). The resonance signal at 13.38 ppm corresponding to the free OH protons is observed, which indicates that the ligand is free from coordination with the metal ion center. After complexation, the  $^1\text{H}$  NMR spectrum of non-side chains

complex (**1**) displays similar resonance signals, integration and splitting patterns to those of the ligand except for the resonance signal at 13.38 ppm corresponding to the free OH protons which is previously observed in the spectrum of the free ligand, and is now absent in the spectrum of the complex. This confirms that deprotonation of the OH groups has occurred due to the coordination of oxygen atoms to the platinum(II) metal ion center. There is also significant difference found in their chemical shifts between the spectra of the ligand and its complex. The singlet resonance signal at 9.19 ppm corresponding to N = C-H imine proton of the complex is shifted downfield compared to its original resonance signal at 8.75 ppm of the free salphen ligand, which also supports the coordination of the nitrogen atoms of the imine groups from the salphen ligand to the platinum(II) metal ion center.  $^{13}\text{C}$  NMR spectrum was assigned using 2D HSQC NMR which displays the exact carbon signal that belongs to a certain proton signal for a simple and easy assignment of carbons. The infrared spectrum of the complex shows absorption bands of azomethine -CH = N-, C-O, C = C aromatic, C-H aromatic and OH functional groups at 1601, 1180–1128, 1581–1440, 3066 and 3368  $\text{cm}^{-1}$ , respectively. The mass spectrum of the complex shows the pseudo-molecular ion  $[\text{M} + \text{Na}]^+$  peak at  $m/z$  564.05. The presence of sodium ion is expected as a result of the mass spectrometer instrument itself. The difference between the theoretical calculation  $\text{C}_{20}\text{H}_{14}\text{N}_2\text{PtO}_4$   $[\text{M} + \text{Na}]^+$  (564.41 a.m.u) and the experimental value was  $\pm 0.36$ . Overall, these results support the coordination of four donor atoms  $\text{N}_2\text{O}_2$  from the salphen ligand to the platinum(II) metal ion center, indicating a square-planar geometry and aromatic rings structure.

The hydroxyl side chains derivatives of this complex were prepared by adding 2-chloro-1-ethanol to obtain *N,N'*-bis-[4-[[1-(2-hydroxyethoxy)] salicylidene]

**Fig. 1** Reaction scheme for the salphen ligand and the non-side chains platinum(II) salphen complex (**1**)



phenylenediamine-platinum(II); hydroxyethoxy side chains complex (2) and 3-chloro-1-propanol to obtain *N,N'*-bis-[4-[[1-(3-hydroxypropoxy)] salicylidene] phenylenediamine-platinum(II); hydroxypropoxy side chains complex (3) respectively. Generally, we are interested to study the effect of longer alkoxy side chains from the hydroxyl derivatives of the platinum(II) complex on the binding affinity to DNA. The reaction schemes for the synthesis of the hydroxyethoxy side chains complex (2) and hydroxypropoxy side chains complex (3) are illustrated in Fig. 2. The  $^1\text{H}$  NMR spectrum of hydroxyethoxy side chains complex (2) displays correct integration and multiplets pattern. The hydroxyethoxy side chains arms were proven to be successfully attached to the platinum(II) salphen complex since the  $^1\text{H}$  NMR spectrum of hydroxyethoxy side chains complex (2) displays the formation of new proton signals around the alkyl region at 3.76 ppm (triplet, 2H,  $-\text{CH}_2$ ), and 4.08 ppm (triplet, 2H,  $-\text{CH}_2$ ). The  $^1\text{H}$  NMR spectrum of hydroxypropoxy side chains complex (3) also displays correct integration and multiplets pattern. The hydroxypropoxy side chains arms were also proven to be successfully attached to the platinum(II) salphen complex since the  $^1\text{H}$  NMR spectrum of hydroxypropoxy side chains complex (3) displays the formation of new proton signals around the alkyl region at 1.90 ppm (quantet, 2H,  $-\text{CH}_2$ ), 3.58 ppm (triplet, 2H,  $-\text{CH}_2$ ), and 4.13 ppm (triplet, 2H,  $-\text{CH}_2$ ). The  $^{13}\text{C}$  NMR spectra of both hydroxyethoxy side chains (2) and hydroxypropoxy side chains (3) complexes display the alkyl carbons after the attachment of hydroxyethoxy side chains arms at 59.85 and 70.20 ppm for hydroxyethoxy side chains complex (2) and hydroxypropoxy side chains arms at 32.32, 57.69 and 65.32 ppm for hydroxypropoxy side chains complex (3).

The infrared spectra of both hydroxyethoxy side chains (2) and hydroxypropoxy side chains (3) complexes show additional new peaks absorption bands at  $2916\text{ cm}^{-1}$  which refer to C-H (alkane) stretching or  $\nu(\text{CH}_2)$  after the addition of the

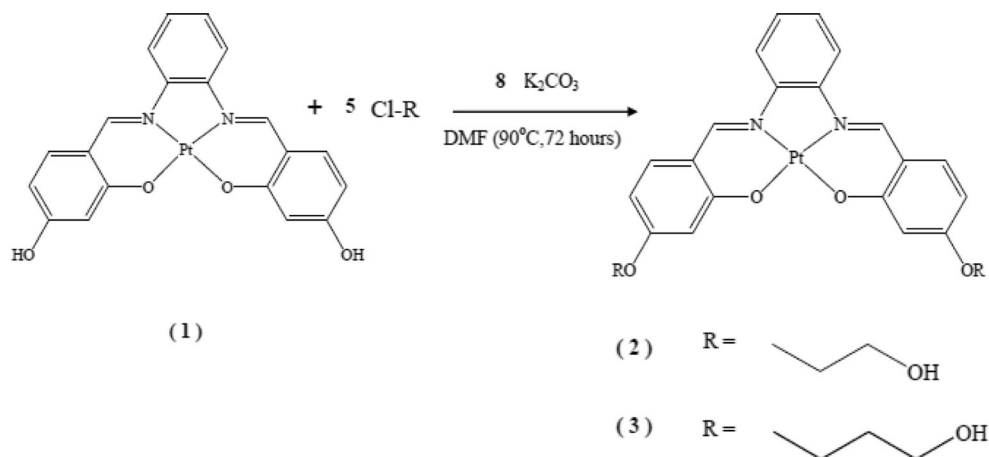
side chain  $-\text{CH}_2\text{CH}_2\text{OH}$  and  $-\text{CH}_2\text{CH}_2\text{CH}_2\text{OH}$  respectively. Moreover, there is also another additional new peaks absorption bands at  $1026\text{ cm}^{-1}$  and  $1024\text{ cm}^{-1}$  for hydroxyethoxy side chains (2) and hydroxypropoxy side chains (3) complexes respectively, which refer to C-O aryl ether stretching  $-\text{ROCH}_2\text{CH}_2\text{OH}$  and  $-\text{ROCH}_2\text{CH}_2\text{CH}_2\text{OH}$  (R = aromatic benzene) after the addition of the hydroxyethoxy and hydroxypropoxy side chains respectively, in which these peaks were absent in the infrared spectrum of the non-side chains complex (1).

The mass spectrum of the hydroxyethoxy side chains (2) complex shows the pseudo-molecular ion  $[\text{M} + \text{K}]^+$  peak at  $m/z$  668.07. The presence of potassium ion is expected as a result of the mass spectrometer instrument itself. The difference between the theoretical calculation  $\text{C}_{24}\text{H}_{22}\text{N}_2\text{PtO}_6$   $[\text{M} + \text{K}]^+$  (668.49 a.m.u.) and the experimental value was  $\pm 0.42$ . Similarly, the mass spectrum of the hydroxypropoxy side chains (3) complex also shows the pseudo-molecular ion  $[\text{M} + \text{K}]^+$  peak at  $m/z$  696.07. The difference between the theoretical calculation  $\text{C}_{26}\text{H}_{26}\text{N}_2\text{PtO}_6$   $[\text{M} + \text{K}]^+$  (696.54 a.m.u.) and the experimental value was  $\pm 0.47$ . Overall, these results indicate that the hydroxyl side chains derivatives of the Pt(II) salphen complex which contain hydroxyethoxy side chains and hydroxypropoxy side chains were successfully obtained. The  $^1\text{H}$  NMR,  $^{13}\text{C}$  NMR, FTIR and ESI-MS spectra for non-side chains (1), hydroxyethoxy side chains (2) and hydroxypropoxy side chains (3) complexes are available in the supplementary information on the Journal's website.

### UV-Vis DNA Titration

The UV-Vis absorption spectra of the non-side chains (1), hydroxyethoxy side chains (2) and hydroxypropoxy side chains (3) complexes show three intense bands at 304–316 nm, 364–368 nm and 421–431 nm (Figs. 3, 4 and 5). The absorption bands at 304–316 nm region are assigned to the intraligand-charge-transfer (ILCT)  $\pi-\pi^*$  transition which involves molecular orbitals localized on the C = N group and

**Fig. 2** Reaction scheme for the hydroxyethoxy side chains platinum(II) salphen complex (2) and hydroxypropoxy side chains platinum(II) salphen complex (3)



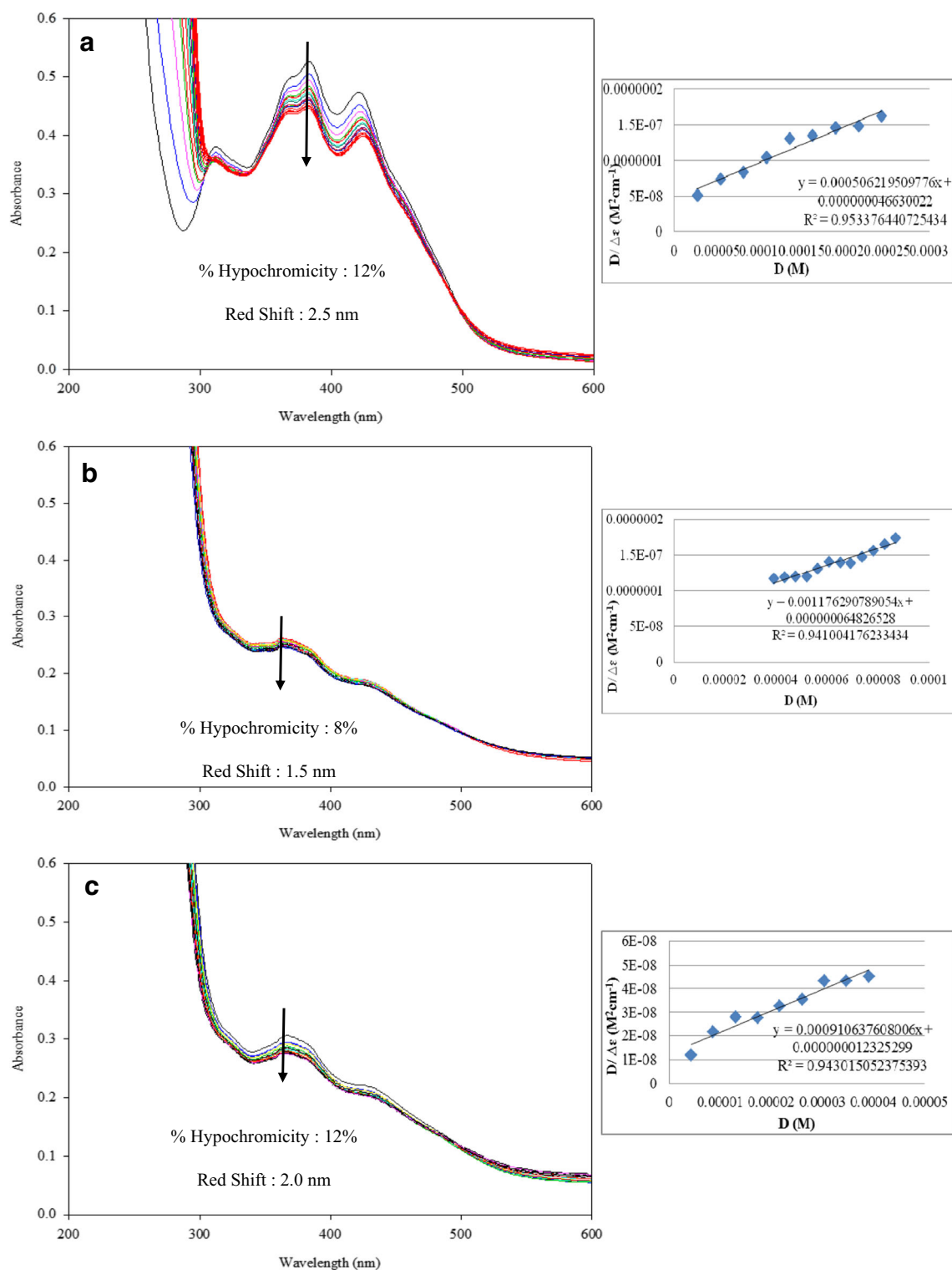


**Fig. 3** Absorption spectral changes of the complexes (30  $\mu\text{M}$ ) in Tris-HCl buffer (pH 7.4) in the absence and presence of increasing concentrations of CT-DNA. The inset graph in the top right corner shows the fitting of the absorbance data that was used to obtain the

binding constant. **a** non-side chains (1) (CT-DNA :  $2.71 \times 10^{-5}$  M -  $4.34 \times 10^{-4}$  M), **(b)** hydroxyethoxy side chains (2) (CT-DNA:  $4.34 \times 10^{-6}$  M -  $7.8 \times 10^{-5}$  M), **(c)** hydroxypropoxy side chains (3) (CT-DNA:  $4.34 \times 10^{-6}$  M -  $7.8 \times 10^{-5}$  M)

the benzene ring. On the other hand, absorption bands in the region of 364–368 nm are assigned to the  $n-\pi^*$  transition involving molecular orbitals of the C = N chromophore and

the benzene ring, while the lowest energy band at 421–431 nm region are attributed to the metal-to-ligand-charge-transfer (MLCT) transition [8].

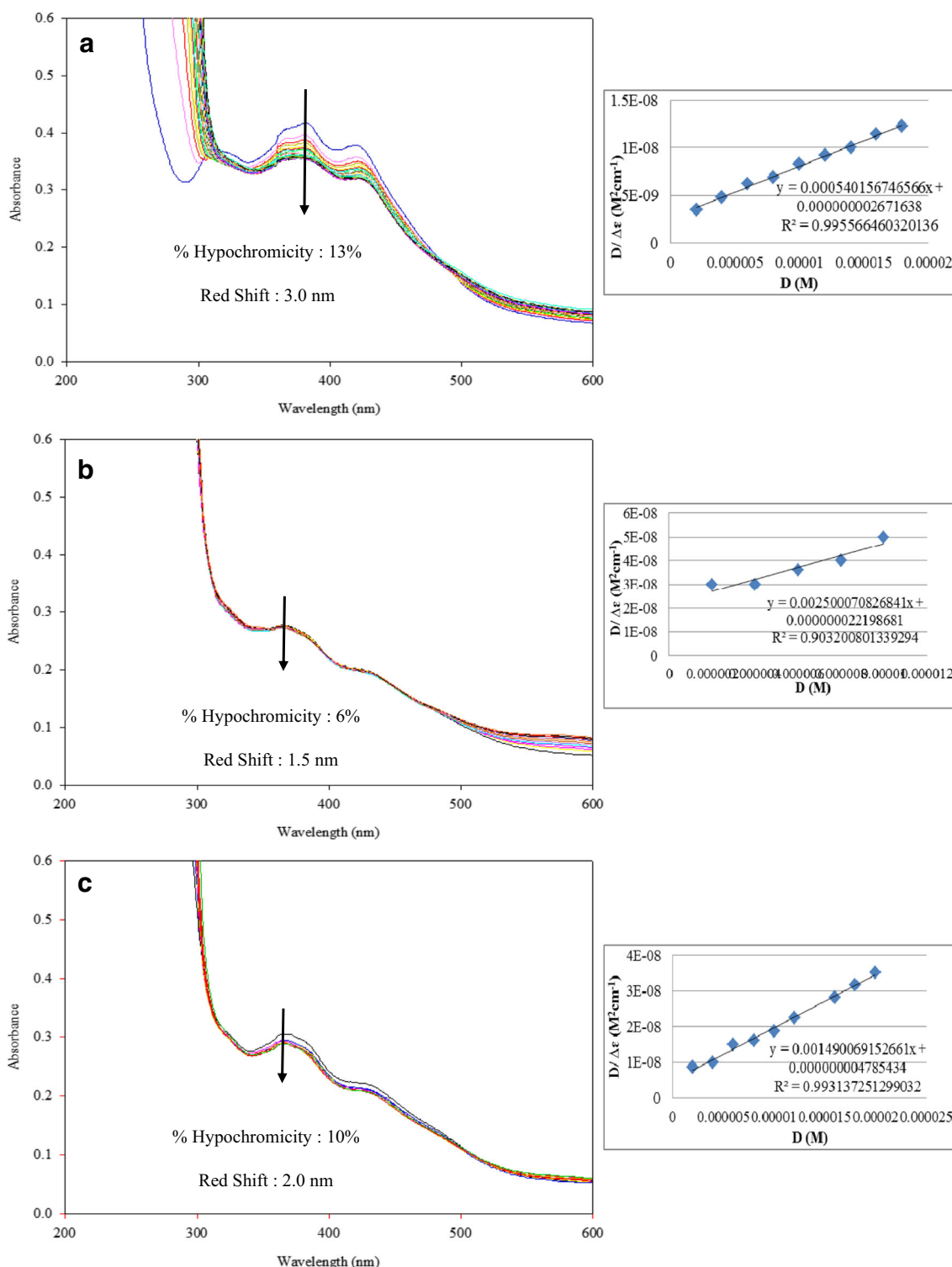


**Fig. 4** Absorption spectral changes of the complexes (30  $\mu\text{M}$ ) in Tris-HCl buffer (pH 7.4) in the absence and presence of increasing concentrations of porcine DNA. The inset graph in the top right corner shows the fitting of the absorbance data that was used to obtain the

binding constant. **a** non-side chains (1) (porcine DNA:  $2 \times 10^{-6}$  M -  $6 \times 10^{-5}$  M), **(b)** hydroxyethoxy side chains (2) (porcine DNA:  $2 \times 10^{-6}$  M -  $6 \times 10^{-5}$  M), **(c)** hydroxypropoxy side chains (3) (porcine DNA:  $2 \times 10^{-6}$  M -  $6 \times 10^{-5}$  M)

In the DNA binding studies, the absorbance measurements were performed using constant complex concentration (30  $\mu\text{M}$ ) while varying the concentration of DNA until

saturation. The spectrum of the complex was recorded after each addition of the respective DNA. Generally, binding of intercalative compounds to DNA can be characterized by

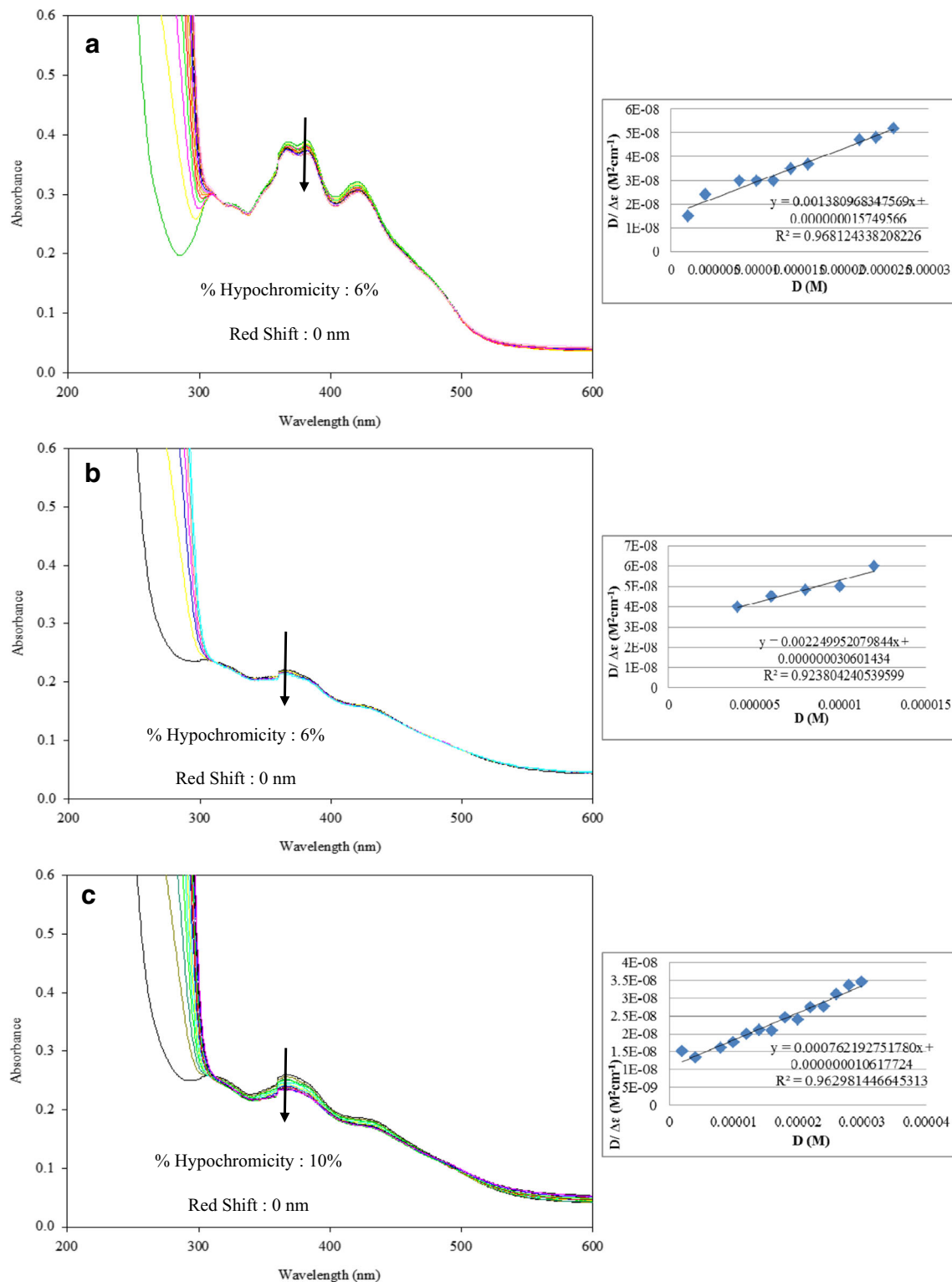


**Fig. 5** Absorption spectral changes of the complexes (30  $\mu$ M) in Tris-HCl buffer (pH 7.4) in the absence and presence of increasing concentrations of single-stranded DNA (beef ssDNA). The inset graph in the top right corner shows the fitting of the absorbance data that was

used to obtain the binding constant. **a** non-side chains (**1**) (beef ssDNA:  $2 \times 10^{-6}$  M -  $2.6 \times 10^{-5}$  M), **(b)** hydroxyethoxy side chains (**2**) (beef ssDNA:  $2 \times 10^{-6}$  M -  $1.2 \times 10^{-5}$  M), **(c)** hydroxypropoxy side chains (**3**) (beef ssDNA:  $2 \times 10^{-6}$  M -  $3 \times 10^{-5}$  M)

absorption spectral titrations where decreased absorbance (hypochromism) and shift to longer wavelengths

(bathochromic shift or red shift) are observed [40]. The hypochromic effect is the spectral characteristics of double helix

DNA due to the contraction of the helix along its axis after insertion of intercalative compound into the DNA double helix. Meanwhile, bathochromic shift or red shift occurs because of the conformational changes of DNA which indicate a new compound “complex-DNA” has been formed [42].

The percentage of hypochromicity can be calculated according to Eq. (1):

$$\% \text{ hyperchromicity} = \frac{\varepsilon_{\text{free}} - \varepsilon_{\text{bound}}}{\varepsilon_{\text{free}}} \times 100 \quad (1)$$

From the UV-Vis DNA titrations, all the complexes exhibit hypochromism (6% -13%) and red shifts (1.5–3 nm) at 364–368 nm region with increasing amounts of DNA (Table 1). These results are in agreement to other established intercalators (hypochromicity =3% - 39%, red shift =1–4 nm) [43] and (hypochromicity =9% - 41%, red shift =1–3 nm) [44].

The intrinsic binding constant  $K_b$  of platinum(II) salphen complex–DNA was determined according to Eq. (2):

$$\frac{\text{DNA}}{\Delta\varepsilon_{\text{ap}}} = \frac{\text{DNA}}{\Delta\varepsilon} + \frac{1}{\Delta\varepsilon \times K_b} \quad (2)$$

where the apparent molar extinction coefficient,  $\Delta\varepsilon_{\text{ap}} = |\varepsilon_A - \varepsilon_F|$ ,  $\varepsilon_A = A_{\text{observed}} / [\text{Complex}]$ ,  $\Delta\varepsilon = |\varepsilon_B - \varepsilon_F|$ .  $\varepsilon_F$  and  $\varepsilon_B$  represent molar extinction coefficients for the free platinum complex and for the DNA bound platinum complex, respectively. In order to elucidate the binding affinity of the complex to DNA, the intrinsic binding constant  $K_b$  was determined by monitoring the changes of maximum absorption bands centred at around 364–368 nm region. From the plotted graph of  $[\text{DNA}]/(\Delta\varepsilon_{\text{ap}})$  versus  $[\text{DNA}]$ , the y-intercept is equal to  $1/(\Delta\varepsilon_{\text{ap}} \times K_b)$  whereas the slope is equal to  $1/\Delta\varepsilon_{\text{ap}}$ .  $K_b$  values can be determined by dividing the slope value by the y-intercept.

To compare quantitatively the binding affinity of the three complexes to DNA, the intrinsic binding constants  $K_b$  of the complexes to duplex CT-DNA were obtained with increasing concentration of DNA. The binding constants ( $K_b$ ) of non-

side chains (1), hydroxyethoxy side chains (2) and hydroxypropoxy side chains (3) complexes with duplex CT-DNA are  $3.21 \times 10^4 \text{ M}^{-1}$ ,  $1.82 \times 10^4 \text{ M}^{-1}$  and  $6.99 \times 10^4 \text{ M}^{-1}$  respectively (Table 1), which is in agreement to other established metal complex intercalators in which the order of magnitude are  $10^4 \text{ M}^{-1}$  [22, 23, 39, 45]. The results showed that hydroxypropoxy side chains complex (3) displays the highest binding affinity with CT-DNA ( $K_b = 6.99 \times 10^4 \text{ M}^{-1}$ ) than the other two complexes. Moreover, hydroxypropoxy side chains complex (3) also exhibit the highest affinity to CT-DNA when comparing the intrinsic binding constants with those of other DNA-intercalative Ru(II) complexes ( $1.1\text{--}4.8 \times 10^4 \text{ M}^{-1}$ ) [23], Co(II) complex ( $3.75 \times 10^4 \text{ M}^{-1}$ ) [22] and Ru(II) complexes ( $3.73\text{--}5.91 \times 10^4 \text{ M}^{-1}$ ) [39]. We can deduce that the non-side chains (1), hydroxyethoxy side chains (2) and hydroxypropoxy side chains (3) complexes bind to CT-DNA by intercalation and that hydroxypropoxy side chains complex (3) binds more strongly than non-side chains (1) and hydroxyethoxy side chains (2) complexes.

Successful porcine DNA sensor should not only interact strongly with their target porcine DNA sequence but also exhibit the highest selectivity for duplex porcine DNA versus other duplex DNA (CT-DNA) and single-stranded DNA (represented by beef ssDNA). Therefore, for comparative purposes the UV-Vis spectroscopic titrations were carried out for all these three DNA to establish whether the complexes have the strongest binding affinity with porcine DNA. The binding constants of all the complexes with duplex porcine DNA are in the order of magnitude  $10^5 \text{ M}^{-1}$  which is in agreement to other metal complex intercalators ( $10^5 \text{ M}^{-1}$ ) [46, 47]. The  $K_b$  values of the non-side chains (1), hydroxyethoxy side chains (2) and hydroxypropoxy side chains (3) complexes with duplex porcine DNA are  $2.21 \times 10^5 \text{ M}^{-1}$ ,  $1.38 \times 10^5 \text{ M}^{-1}$  and  $3.06 \times 10^5 \text{ M}^{-1}$  respectively. Again, hydroxypropoxy side chains complex (3) displays the highest binding affinity with duplex porcine DNA ( $K_b = 3.06 \times 10^5 \text{ M}^{-1}$ ) than the other two complexes. Meanwhile, the  $K_b$  values of the complexes with single-stranded beef DNA are in the

**Table 1** Summary of binding affinity of non-side chains (1), hydroxyethoxy side chains (2) and hydroxypropoxy side chains (3) complexes with duplex CT-DNA, duplex porcine DNA and single-stranded DNA (beef ssDNA)

Complex	CT-DNA $K_b$ ( $\text{M}^{-1}$ ) dsDNA	PORCINE $K_b$ ( $\text{M}^{-1}$ ) dsDNA	BEEF $K_b$ ( $\text{M}^{-1}$ ) ssDNA
Non-Side Chains (1) (368 nm)	$K_b$ : $3.21 \times 10^4 \pm 3.00$ % Hypochromicity: 12% Red Shift: 2.5 nm	$K_b$ : $2.21 \times 10^5 \pm 0.26$ % Hypochromicity: 13% Red Shift: 3.0 nm	$K_b$ : $8.56 \times 10^4 \pm 0.30$ % Hypochromicity: 6% Red Shift: 0 nm
Hydroxyethoxy Side Chains (2) (364 nm)	$K_b$ : $1.82 \times 10^4 \pm 0.01$ % Hypochromicity: 8% Red Shift: 1.5 nm	$K_b$ : $1.38 \times 10^5 \pm 0.35$ % Hypochromicity: 6% Red Shift: 1.5 nm	$K_b$ : $7.35 \times 10^4 \pm 0.01$ % Hypochromicity: 6% Red Shift: 0 nm
Hydroxypropoxy Side Chains (3) (368 nm)	$K_b$ : $6.99 \times 10^4 \pm 0.57$ % Hypochromicity: 12% Red Shift: 2.0 nm	$K_b$ : $3.06 \times 10^5 \pm 0.07$ % Hypochromicity: 10% Red Shift: 2.0 nm	$K_b$ : $7.27 \times 10^4 \pm 0.12$ % Hypochromicity: 10% Red Shift: 0 nm

order of magnitude  $10^4 \text{ M}^{-1}$ . Although the  $K_b$  values with the beef ssDNA are in the same magnitude as the duplex CT-DNA ( $10^4 \text{ M}^{-1}$ ), there were no red shifts for beef ssDNA unlike those observed for duplex CT-DNA and duplex porcine DNA. Therefore, beef ssDNA probably exhibit a binding mode other than intercalation such as electrostatic binding or groove binding (surface binding) [48, 49]. Best selectivity towards duplex porcine DNA ( $K_b = 10^5 \text{ M}^{-1}$ ) over single-stranded DNA (beef ssDNA,  $K_b = 10^4 \text{ M}^{-1}$ ) and duplex CT-DNA ( $K_b = 10^4 \text{ M}^{-1}$ ) was obtained by one order of magnitude higher for the porcine DNA. Therefore, from the binding constants obtained from the three DNA, it can be concluded that the highest binding affinity and selectivity towards duplex porcine DNA is established.

Moreover, it was observed that the addition of the increasing lengths of the alkoxy side chains arms of the hydroxyl derivatives can reduce the binding strength of the complexes to the single-stranded DNA compared to the non-side chains complex (**1**). For instance, the non-side chains complex (**1**) has the strongest binding strength ( $K_b = 8.56 \times 10^4 \text{ M}^{-1}$ ) with single-stranded beef DNA. Meanwhile, hydroxyethoxy side chains complex (**2**) with the shorter hydroxyl functionalized alkoxy side chains arms have a weaker DNA binding ( $K_b = 7.35 \times 10^4 \text{ M}^{-1}$ ) while hydroxypropoxy side chains complex (**3**) with the longer alkoxy side chains arms has the most weakest DNA binding ( $K_b = 7.27 \times 10^4 \text{ M}^{-1}$ ), thus making it most selective to porcine dsDNA.

From the above results in general, hydroxypropoxy side chains complex (**3**) with the longer alkoxy side chains [Hydroxypropoxy] arms seem to have the highest binding affinity to both CT-DNA and porcine DNA. Therefore, we can summarize that the highest degree of binding affinity of all the complexes to both duplex porcine DNA and CT-DNA are in the order of complex hydroxypropoxy side chains (**3**) > non-side chains (**1**) > hydroxyethoxy side chains (**2**). Moreover, hydroxypropoxy side chains complex (**3**) also has the weakest binding affinity with single-stranded beef DNA compared to the other two complexes, which succeeded our aim to have a lower binding with single-stranded DNA as much as possible while achieving the highest binding affinity with target duplex porcine DNA. In the design of duplex porcine DNA sensor it is highly desirable to reduce the binding affinity of the complex to single-stranded DNA so as to increase the selectivity for target duplex porcine DNA versus non-target single-stranded DNA.

The UV-Vis DNA titration results show that there is an interaction between the electronic states of the chromophores in the salphen conjugates with DNA [1]. This complex can intercalate with the conjugated DNA bases due to its planar structures and aromatic rings structure. Square-planar geometry can give planar structures, hence the planarity can provide a suitable environment for insertion between the conjugated base pairs of the DNA double helix during intercalation [38].

The observed spectroscopic characteristics suggest that the complex interacts with duplex CT-DNA and duplex porcine DNA through a mode that involves a  $\pi$ - $\pi$  stacking interaction between the aromatic rings of salphen and the base pairs of DNA. Our results support the theory of Liu & Sadler [38], which states that the square-planar platinum(II) complexes containing heterocyclic aromatic ligands non-covalently bind to DNA duplexes by intercalating between the base pairs. Remarkably, the attachment of [Hydroxypropoxy] side chains arms to the platinum(II) salphen complex can increase the binding affinity of the complex to DNA and is the best DNA binder among the other two complexes.

### Emission DNA Titration

All the compounds have been tested with different wavelength with reference to the lambda maximum obtained in the UV-VIS spectrums of the compounds. However, only the excitation wavelength of 370 nm gives the highest and strongest emission signals intensities for all the compounds. Therefore, it was chosen as the best excitation wavelength and this excitation wavelength was used for all the compounds.

The same optical alignment was used for all samples throughout the experiments. Moreover, the baseline signals were first recorded and have been normalized. We have done the baseline without the DNA, without the metal complex, and found that the emission signals obtained were due to the effect of the excitation at that certain wavelength.

The complexes emit phosphorescence emission at 570 nm when excited at 370 nm in DMSO solvent. The intensity of the emission in DMSO solvent for non-side chains (**1**), hydroxyethoxy side chains (**2**) and hydroxypropoxy side chains (**3**) complexes (30  $\mu\text{M}$ ) are 160, 130 and 130 respectively (Supplementary data, Fig. S15). In order to conduct emission DNA titration and to study the effect of the increasing amount of DNA on the phosphorescence properties of the complex, the complexes must be diluted in Tris-HCl buffer (30% DMSO, 70% buffer). In Tris-HCl buffer, the phosphorescence emission intensity for non-side chains (**1**), hydroxyethoxy side chains (**2**) and hydroxypropoxy side chains (**3**) complexes are 9, 66 and 65 respectively (Fig. 6). Non-side chains complex (**1**) seems to have the lowest emission and this is probably because the complex is very sensitive to the presence and concentration of water, being almost quenched completely (Intensity: 9) in the aqueous solution of Tris-HCl buffer. This phenomenon is similar to the Ru(II) complexes which showed the progressive decrease of the emission intensity in MeCN upon the addition of  $\text{H}_2\text{O}$  [23]. A similar effect of the emission properties was also observed for  $[\text{Ru}(\text{phen})_2(\text{qdppz})]^{2+}$  which was non-luminescence in aqueous MeCN (10%  $\text{H}_2\text{O}$ ) [50]. Therefore, the lack of luminescence in water or Tris-HCl buffer for non-side chains

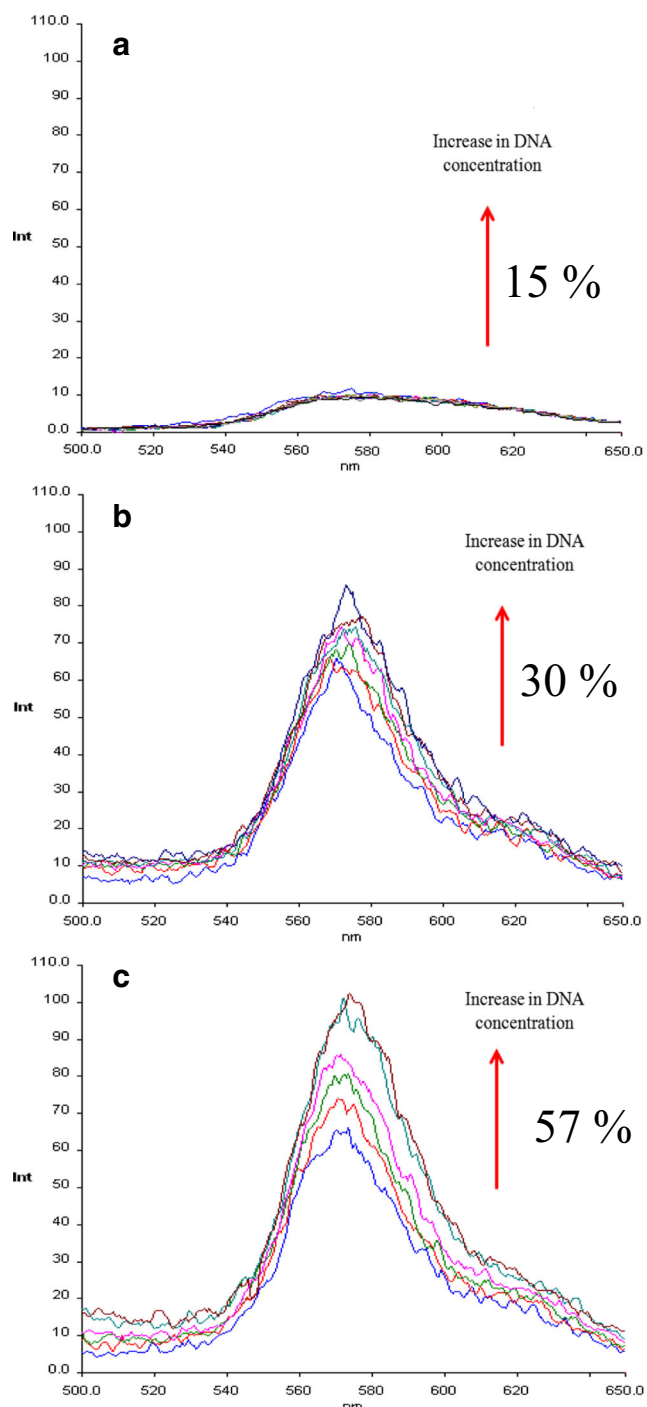


**Fig. 6** Phosphorescence emission spectra of the platinum(II) salen complexes ( $30 \mu\text{M}$ ) in the Tris-HCl buffer (pH 7.4) in the absence and presence of increasing concentrations of porcine DNA ( $2 \times 10^{-6} \text{ M}$  to  $6 \times 10^{-5} \text{ M}$ ).  $\lambda$  excitation =  $370 \text{ nm}$ .  $\lambda$  emission =  $570 \text{ nm}$ . The slit width was  $5 \text{ nm}$  for both excitation and emission, with a scan rate of  $200 \text{ nm/min}$ . (a) non-side chains (1), (b) hydroxyethoxy side chains (2), (c) hydroxypropoxy side chains (3)

complex (1) maybe due to the mechanism similar to that of the ruthenium complex mentioned above. This observation is also consistent with  $\text{Pt}(\text{trpy})\text{OH}^+$  which showed no significant emission in water due to solvent effects that elevate the energy

of the charge-transfer (CT) state and facilitate deactivation via metal-centered excited state [51].

Emission titration experiments were performed using a constant complex concentration ( $30 \mu\text{M}$ ) and varying the porcine DNA concentration (from  $2 \times 10^{-6} \text{ M}$  to  $6 \times 10^{-5} \text{ M}$ ), where the ratio of complex to the porcine DNA is 1:2. The addition of increasing amounts of porcine DNA to non-side chains (1), hydroxyethoxy side chains (2) and hydroxypropoxy side chains (3) complexes showed a significant marked increase in the phosphorescence intensity with the emission enhancement value of 1.15 (15%), 1.30 (30%) and 1.57 (57%) times larger respectively, which indicate the interaction of the complexes with porcine DNA (Fig. 6). Higher emission enhancements were observed for the hydroxyl substituent hydroxyethoxy side chains (2) and hydroxypropoxy side chains (3) complexes compared to the non-side chains complex (1). Moreover, the values of emission enhancement for hydroxyethoxy side chains (2) and hydroxypropoxy side chains (3) complexes are similar to those observed for other Ru(II) complexes DNA-intercalators in which the emission intensities were enhanced by 1.3–1.6 times higher [52] than those in the absence of DNA. The emission enhancements indicate that the complexes can strongly interact with DNA and can be protected from solvent water molecules by the hydrophobic environment inside the DNA helix [45], with hydroxypropoxy side chains complex (3) being protected more efficiently than hydroxyethoxy side chains (2) and non-side chains (1) complexes. This suggest that the complexes can insert between DNA bases deeply and that hydroxypropoxy side chains complex (3) can bind to DNA more strongly than the other two complexes, since the hydrophobic environment inside the DNA helix reduces the accessibility of solvent water molecules to the complex and the complex mobility is restricted at the binding site, which leads to the decrease of the vibrational modes of relaxation [39, 52]. The binding of the compounds to DNA leading to a significant increase of emission intensity also agrees with those observed for other typical intercalators [43]. Nyarko et al. also reported the same phenomenon for  $\text{Pd}(\text{II})(\text{TMPyP})^{4+}$  and  $\text{Pt}(\text{II})(\text{TMPyP})^{4+}$  complexes where the increased phosphorescence and fluorescence emission in the presence of DNA was due to the shielding of the intercalated porphyrin by the DNA thus preventing it from reacting with molecular oxygen dissolved in water [53]. In addition, it was reported that if the complex interacts with DNA through classical intercalation, the emission intensity increases as the complex gets into a hydrophobic environment inside DNA. Considering all of these factors, it is suggested that the complex does bind to DNA by a classical intercalative mode [22, 46]. The highest phosphorescence enhancements are in the order of complex hydroxypropoxy side chains (3) > hydroxyethoxy side chains (2) > non-side chains (1). Since hydroxypropoxy side chains complex (3) can bind to

duplex porcine DNA more strongly than the other two complexes, and also displays the highest value of emission enhancement, therefore hydroxypropoxy side chains complex (3) is the best candidate chosen as an optical phosphorescent indicator for porcine DNA biosensor among the three complexes.

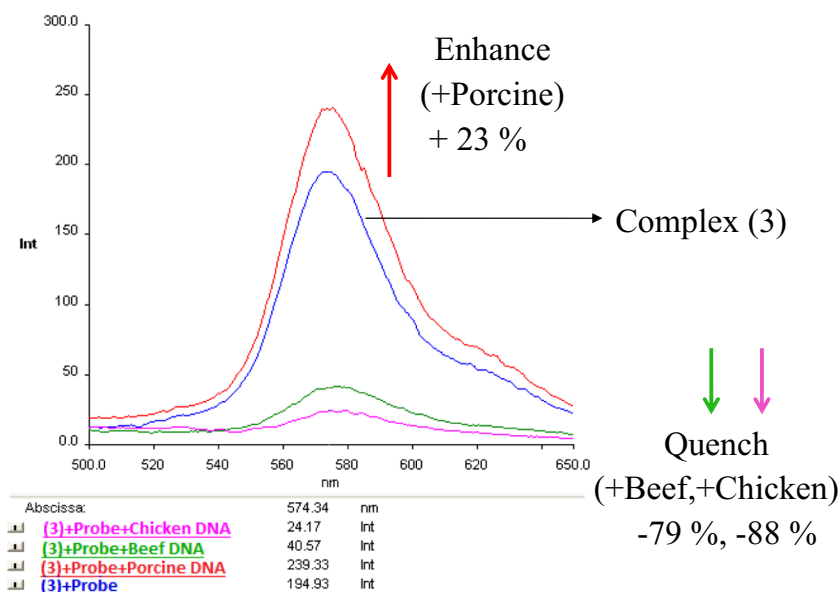
### Preliminary DNA Selectivity Sensor Solution Study with Porcine, Beef and Chicken DNA

The sensor solution study of the chosen hydroxypropoxy side chains complex (3) was conducted to investigate its selectivity to the complimentary (target porcine ssDNA) versus non-complimentary (beef and chicken ssDNA). 1 mM of hydroxypropoxy side chains complex (3) was prepared in THF-Tris HCl buffer solution (30% THF, 70% buffer) and the concentration of the probe porcine DNA and the complimentary or non-complimentary DNA were both fixed at 4  $\mu$ M. Three vials tubes of 1 mM of hydroxypropoxy side chains complex (3) were prepared with each tube containing porcine DNA probe. The vials were then added with complimentary (target porcine DNA), non-complimentary (beef DNA), and non-complimentary (chicken DNA) separately in each tubes. All the vials tubes were annealed at 90  $^{\circ}$ C for 5 min, then cooled to 50  $^{\circ}$ C for 1 h to allow perfectly matched annealing (hybridization) of the complimentary DNA and the mismatched non-annealing (non-hybridization) of the non-complimentary DNA [13].

The complimentary target porcine DNA signal displays a phosphorescence “enhancement” (increased by 23%), while both non-complimentary DNA signals were “quenched” for beef DNA (decreased by 79%) and chicken DNA (decreased by 88%) (Fig. 7). The enhanced emission signal of the complimentary target porcine DNA was attributed to the

hydrophobic environment of the DNA and the subsequent intercalation of hydroxypropoxy side chains complex (3) into the DNA bases as mentioned previously. Any emissive DNA intercalator will be able to show the response reported in the main figure of the manuscript (Fig. 7). Meanwhile the quenching effect or the decreased emission intensity for the non-complimentary DNA (beef and chicken DNA) was probably due to self-stacking of some free bases in the compound along DNA surface [46, 53]. The same phenomenon was also observed for electrostatic binding mode of cobalt(II) Schiff base complex where the emission decrease with the addition of DNA [48]. In addition, the emission quenching could also be due to the photoelectron transfer from the guanine base of DNA to the excited MLCT state of the complex as observed by [Co(bzimpy)<sub>2</sub>], [Ru(bzimpy)<sub>2</sub>]<sup>2+</sup>, [Ru(TAP)<sub>3</sub>]<sup>2+</sup> and Pt(trpy)OH<sup>+</sup> complexes [49, 51, 54, 55]. The mismatch beef and chicken DNA cannot form duplex DNA since they are not complimentary to the probe porcine DNA, therefore no hybridization and intercalation of the complex can happen and only single-stranded DNA were present. As a consequence, the complex cannot be protected by the hydrophobic environment from the hybridized duplex DNA, thus giving rise to other modes of DNA binding with the single-stranded non-complimentary DNA such as electrostatic binding or groove binding and at the same time allowing the complex to interact with the free guanine bases that can act as a quencher. Because of the differences in the phosphorescence spectral characteristic of the complex when interacted with DNA, this will allow for an easy and rapid sensor method to detect and distinguish porcine DNA among the different DNA, where the complimentary (target porcine DNA) signal will be enhanced while the non-complimentary signals will be quenched. Since the complex showed selectivity for hybridized duplex porcine DNA over non-hybridized single-stranded DNA, these

**Fig. 7** Phosphorescence emission spectra for sensor selectivity solution study of hydroxypropoxy side chains complex (3) (1 mM) in THF-Tris-HCl buffer (pH 7.4) with different DNA (porcine, beef, chicken) (4  $\mu$ M).  $\lambda$  excitation =370 nm.  $\lambda$  emission =574 nm. The slit width was 5 nm for both excitation and emission, with a scan rate of 200 nm/min



findings will be valuable for the potential use of hydroxypropoxy side chains platinum(II) salphen complex **(3)** as an optical porcine DNA indicator sensor material for the detection of porcine DNA in food products. Current work on fabrication of this phosphorescence metal complex as an optical indicator sensor material for porcine DNA biosensors and incorporating this optical indicator into a polymer matrix, which is then deposited on solid support sensors are undergoing in our laboratory.

## Conclusions

The platinum(II) salphen complex *N,N'*-Bis-4-(hydroxysalicylidene)-phenylenediamine-platinum(II); non-side chains **(1)** and its two hydroxyl substituent with varying lengths of the alkoxy side chain arms *N,N'*-bis-[4-[[1-(2-hydroxyethoxy)] salicylidene] phenylenediamine-platinum(II); hydroxyethoxy side chains **(2)** and *N,N'*-bis-[4-[[1-(3-hydroxypropoxy)] salicylidene] phenylenediamine-platinum(II); hydroxypropoxy side chains **(3)** were synthesized and characterized by spectroscopic methods. All the complexes interact with duplex CT-DNA and porcine DNA via the intercalation mechanism. These platinum(II) complexes can intercalate with the conjugated DNA bases due to its square-planar and aromatic rings structure. The UV-Vis DNA titration showed the highest binding affinity of *N,N'*-bis-[4-[[1-(3-hydroxypropoxy)] salicylidene] phenylenediamine-platinum(II); hydroxypropoxy side chains **(3)** to DNA compared to the other two complexes. The degree of binding affinity for all the platinum(II) complexes to DNA are in the order of complex hydroxypropoxy side chains **(3)** > non-side chains **(1)** > hydroxyethoxy side chains **(2)**. Higher selectivity for duplex porcine DNA over single-stranded DNA and also CT-DNA was achieved. Moreover, an enhancement of phosphorescence emission intensity by 57% upon the addition of porcine DNA suggests that hydroxypropoxy side chains complex **(3)** has the most potential as an optical phosphorescence porcine DNA biosensor. The sensor solution study of hydroxypropoxy side chains complex **(3)** showed a good selectivity towards complementary target porcine DNA, allowing for an easy and rapid sensor method to detect and distinguish porcine DNA among the different DNA. The use of this phosphorescence metal complex as an optical porcine DNA indicator sensor material in solid sensors is currently undergoing in our laboratory. These findings will be valuable for the potential use of the hydroxypropoxy side chains platinum(II) salphen complex **(3)** as an optical indicator sensor material for porcine DNA biosensor, contributing to an easy, simpler, and rapid alternative method to detect porcine DNA in food samples for an improved food industry analysis method in the future.

**Acknowledgements** The authors would like to acknowledge Universiti Kebangsaan Malaysia (UKM) for providing the research facilities and grant funding 06-01-02-SF0898, GGPM-2012-074 and FRGS/1/2013/ST01/UKM/03/2 for financial support throughout this research.

## References

- Mariappan M, Suenaga M, Mukhopadhyay A (2012) Synthesis, structure, DNA binding and photonuclease activity of a nickel(II) complex with a *N,N'*-Bis(salicylidene)-9-(3,4-diaminophenyl)acridine ligand. *Inorg Chim Acta* 390:95–104
- Wu H, Sun T, Li K, Liu B, Kou F, Jia F, Yuan J, Bai Y (2012) Synthesis, crystal structure, and DNA-binding studies of a nickel(II) complex with the bis(2-benzimidazolymethyl)amine ligand. *Bioinorg Chem Appl* 609796. doi:10.1155/2012/609796
- Vilar R, Arola-Amal A, Benet-Buchholz J, Neidle S (2008) Effects of metal coordination geometry on stabilization of human telomeric quadruplex DNA by square-planar and square-pyramidal metal complexes. *Inorg Chem* 47:11910–11919
- Campbell NH, Karim NHA, Parkinson GN, Gunaratnam M, Petrucci V, Todd AK, Vilar R, Neidle S (2012) Molecular basis of structure–activity relationships between salphen metal complexes and human telomeric DNA Quadruplexes. *J Med Chem* 55(1):209–222
- Karim NHA, Mendoza O, Shivalingam A, Thompson AJ, Ghosh S, Kuimova MK, Vilar R (2014) Salphen metal complexes as tunable G-quadruplex binders and optical probes. *RSC Adv* 4:3355–3363
- Bhattacharya S, Mandal SS (1995) Ambient oxygen activating water soluble cobalt–salen complex for DNA cleavage. *J Chem Soc Chem Comm* 33:2489–2490
- Arjmand F, Sayeed F, Muddassir M (2011) Synthesis of new chiral heterocyclic Schiff base modulated Cu(II)/Zn(II) complexes: their comparative binding studies with CT-DNA, mononucleotides and cleavage activity. *J Photochem Photobiol B Biol* 103:166–179
- Zhou L, Feng Y, Cheng J, Sun N, Zhou X, Xiang H (2012) Simple, selective, and sensitive colorimetric and ratiometric fluorescence/phosphorescence probes for platinum(II) based on salen-type Schiff bases. *RSC Adv* 2:10529–10536
- Wu W, Sun J, Ji S, Zhao J, Guo H (2011) Tuning the emissive triplet excited states of platinum(II) Schiff base complexes with pyrene, and application for luminescent oxygen sensing and triplet–triplet-annihilation based upconversions. *Dalton Trans* 40:11550–11561
- Baldo MA, Brien DFO, You Y, Shoustikov A, Sibley S, Thompson ME, Forrest SR (1998) Highly efficient phosphorescent emission from organic electroluminescent devices. *Nature* 395:151–154
- Farrokhi R, Joozan RJ (2011) Identification of pork genome in commercial meat extracts for halal authentication by SYBR green I real-time PCR. *Int J Food Science & Tech* 46:951–955
- Tanabe S, Miyauchi E, Muneshige A, Mio K, Sato C, Sato M (2007) PCR Method of Detecting Pork in Foods for Verifying Allergen Labeling and for Identifying Hidden Pork Ingredients in Processed Foods. *Biosci. Biotechnol. Biochem* 71(7):1663–1667
- Ali ME, Hashim U, Mustafa S, Che Man YB, Islam Kh N (2012) Gold nanoparticle sensor for the visual detection of pork adulteration in meatball formulation. *J Nanomater* 103607. doi:10.1155/2012/103607
- Ahmed MU, Hasan Q, Hossain MM, Saito M, Tamiya E (2010) Meat species identification based on the loop mediated isothermal amplification and electrochemical DNA sensor. *Food Control* 21(5):599–605
- Peng Y, Zhong H, Chen ZF, Liu YC, Zhang GH, Qin QP, Liang H (2014) A planar Schiff Base platinum(II) complex: crystal structure,

- cytotoxicity and interaction with DNA. *Chem Pharm Bull* 62(3): 221–228
16. Zhao XL, Ma YZ, Wang KZ (2012) Synthesis, pH-induced “on-off-on” luminescence switching, and partially intercalative DNA-binding and DNA photocleavage properties of an  $\beta$ -D-allopyranoside-grafted ruthenium(II) complex. *J Inorg Biochem* 113:66–76
  17. Erkkila KE, Odom DT, Barton JK (1999) Recognition and reaction of metallointercalators with DNA. *Chem Rev* 99:2777–2796. doi:10.1021/CR9804341
  18. Metcalfe C, Thomas JA (2003) Kinetically inert transition metal complexes that reversibly bind to DNA. *Chem Soc Rev* 32:215–224. doi:10.1039/B201945K
  19. Xiong Y, Ji LN (1999) Synthesis, DNA-binding and DNA-mediated luminescence quenching of Ru(II) polypyridine complexes. *Coord Chem Rev* 185:711–733. doi:10.1016/S0010-8545(99)00019-3
  20. Friedman AE, Chambron JC, Sauvage JP, Turro NJ, Barton JK (1990) A molecular light switch for DNA: Ru(bpy)<sub>2</sub>(dppz)<sup>2+</sup>. *J Am Chem Soc* 112:4960
  21. Jin L, Yang P (1997) Synthesis and DNA binding studies of cobalt(III) mixed-polypyridyl complex. *J Inorg Biochem* 68:79–83
  22. Song YF, Yang P (2001) Mononuclear tetrapyrrodo[3,2-a:2',3'-c:3'',2''-h:2''',3'''-j]phenazine (tpphz) cobalt complex. *Polyhedron* 20: 501–506
  23. Zou XH, Ye BH, Li H, Zhang QL, Chao H, Liu JG, Ji LN, Li XY (2001) The design of new molecular “light switches” for DNA. *J Biol Inorg Chem* 6(2):143–150
  24. Krause-Heuer AM, Grant MP, Orkey N, Aldrich-Wright JR (2008) Drug delivery devices and targeting agents for platinum(II) anticancer complexes. *Aust J Chem* 61:675–681
  25. Tan L, Zhang S, Liu X, Xiao Y (2008) Synthesis, characterization, DNA binding, and photocleavage of [Ru(bpy)<sub>2</sub>(MFIP)]<sup>2+</sup> and [Ru(phen)<sub>2</sub>(MFIP)]<sup>2+</sup>. *Aust J Chem* 61:725–731
  26. Tan L, Chao H, Fei J, Su G, Zhang S, Xia Y, Ji L (2008) DNA-binding and photocleavage behavior of [Ru(bpy)<sub>2</sub>(MDPZ)]<sup>2+</sup>. *Aust J Chem* 61:376–381
  27. Westerlund F, Lincoln P (2007) AT-dependent luminescence of DNA-threading ruthenium complexes. *Biophys Chem* 129:11–17
  28. Westerlund F, Eng MP, Winters MU, Lincoln P (2007) Binding geometry and Photophysical properties of DNA-threading binuclear ruthenium complexes. *J Phys Chem B* 111:310–317
  29. Hiort C, Lincoln P, Norden B (1993) DNA binding of  $\Delta$ - and  $\Lambda$ -[Ru(phen)<sub>2</sub>DPPZ]<sup>2+</sup>. *J Am Chem Soc* 115:3448–3454
  30. Wang YM, Pang XP, Zhang YY (2009) Recent advances in fiber-optic DNA biosensors. *J. Biomedical Science and Engineering* 2: 312–317
  31. Shi S, Wang X, Sun W, Wang X, Yao T, Ji L (2013) Label-free fluorescent DNA biosensors based on metallointercalators and nanomaterials. *Methods* 64:305–314
  32. Piuanno PAE, Krull UJ, Hudson RHE, Damha MJ, Cohen H (1994) Fiber optic biosensor for fluorometric detection of DNA hybridization. *Anal Chim Acta* 288:205–214
  33. Piuanno PAE, Krull UJ, Hudson RHE, Damha MJ, Cohen H (1995) Fiber optic DNA sensor for fluorometric nucleic acid determination. *Anal Chem* 67:2635–2643
  34. Wang X, Krull UJ (2002) Tethered thiazole orange intercalating dye for development of fibre-optic nucleic acid biosensors. *Anal Chim Acta* 470:57–70
  35. Wang X, Krull UJ (2005) A self-contained fluorescent fiber optic DNA biosensor. *J Mater Chem* 15:2801–2809
  36. Suman KA (2008) Recent advances in DNA biosensor. *Sensors & Transducers Journal* 92(5):122–133
  37. Abel AP, Weller MG, Duveneck GL, Ehrat M, Widmer HM (1996) Fiber-optic evanescent wave biosensor for the detection of oligonucleotides. *Anal Chem* 68(17):2905–2912
  38. Liu HK, Sadler PJ (2011) Metal complexes as DNA intercalators. *Acc Chem Res* 44(5):349–359
  39. Xu H, Zheng KC, Lin LJ, Li H, Gao Y, Ji L.N (2004) Effects of the substitution positions of Br group in intercalative ligand on the DNA-binding behaviors of Ru(II) polypyridyl complexes. *J Inorg Biochem* 98: (1) 87–97
  40. Kashanian S, Shahabadi N, Mahdavi M, Sourinejad N (2007) DNA interaction with Al–N,N'-bis(salicylidene)2,2'-phenyldiamine complex. *Spectrochim Acta A* 67:472–478
  41. Chetana PR, Rao R, Roy M, Patra AK (2009) New ternary copper(II) complexes of l-alanine and heterocyclic bases: DNA binding and oxidative DNA cleavage activity. *Inorg Chim Acta* 362(13):4692–4698
  42. Pravinand N, Raman N (2013) DNA interaction and antimicrobial activity of novel tetradentate imino-oxalato mixed ligand metal complexes. *Inorg Chem Commun* 36:45–50
  43. Cheng XY, Wang MF, Yang ZY, Li Y, Liu ZC, Zhou QX (2013) Synthesis, Characterization, Crystal Structure, and Biological Activities of Transition Metal Complexes with 1-Phenyl-3-methyl-5-hydroxypyrazole-4-methylene-8'-quinolineimine. *Z. Anorg. Allg. Chem* 639(5):832–841
  44. Li Y, Yang ZY, Liao ZC, Han ZC, Liu ZC (2010) Synthesis, crystal structure, DNA binding properties and antioxidant activities of transition metal complexes with 3-carbaldehyde-chromone semicarbazone. *Inorg Chem Commun* 13:1213–1216
  45. Devi CS, Nagababu P, Reddy VV, Sateesh V, Srishailam A, Satyanarayana S (2014) Synthesis, characterisation, interaction with DNA, cytotoxicity, and apoptotic studies of ruthenium(II) polypyridyl complexes. *Aust J Chem* 67:225–233
  46. Rad FV, Housaindokht MR, Jalal R, Hosseini HE, Doghaei AV, Goghari SS (2014) Spectroscopic and molecular modeling based approaches to study on the binding behavior of DNA with a copper (II) complex. *J Fluoresc* 24(4):1225–1234
  47. Raman N, Sobha S, Selvaganapathy M (2012) Probing the DNA-binding behavior of tryptophan incorporating mixed-ligand complexes. *Monatshefte für Chemie-Chemical Monthly* 143(11): 1487–1495
  48. Shahabadi N, Kashanian S, Darabi F (2010) DNA binding and DNA cleavage studies of a water soluble cobalt(II) complex containing dinitrogen Schiff base ligand: the effect of metal on the mode of binding. *Eur J Med Chem* 45:4239–4245
  49. Vaidyanathan VG, Nair BU (2002) Synthesis, characterization and DNA binding studies of a ruthenium(II) complex. *J Inorg Biochem* 91:405–412
  50. Arounaguirri S, Maiya BG (1999) “Electro-Photo Switch” and “Molecular Light Switch” Devices Based on Ruthenium(II) Complexes of Modified Dipyridophenazine Ligands: Modulation of the Photochemical Function through Ligand Design. *Inorg. Chem.* 38(5):842–843
  51. Peyratout CS, Aldridge TK, Crites DK, McMillin DR (1995) DNA-Binding Studies of a Bifunctional Platinum Complex That Is a Luminescent Intercalator. *Inorg. Chem.* 34(17):4484–4489
  52. He X, Yang G, Sun X, Xie L, Tan L (2013) Synthesis and characterisation of Ru(II) polypyridyl complexes: DNA-binding, photocleavage, and topoisomerase I and II inhibitory activity. *Aust J Chem* 66:1406–1414
  53. Nyarko E, Hanada N, Habib A, Tabata M (2004) Fluorescence and phosphorescence spectra of Au(III), Pt(II) and Pd(II) porphyrins with DNA at room temperature. *Inorg Chim Acta* 357:739–745
  54. Vaidyanathan VG, Nair BU (2003) Photooxidation of DNA by a cobalt(II) tridentate complex. *J Inorg Biochem* 94:121–126
  55. Kelly JM, McConnell DJ, OhUigin C, Tossi AB, Mesmaeker AKD, Masschelein A, Nasielski J (1987) Ruthenium polypyridyl complexes; their interaction with DNA and their role as sensitizers for its photocleavage. *J. Chem. Soc., Chem Commun* 1821–1823